ELSEVIER

Biochimica et Biophysica Acta 1274 (1996) 31–38

BBA Biochimica et Biophysica Acta

Size-distributions of antenna and acceptor-pool of Photosystem II

Petra W. Hemelrijk, Hans J. van Gorkom *

Department of Biophysics, Huygens Laboratory of the State University, P.O. Box 9504, NL-2300 RA Leiden, The Netherlands

Received 25 October 1995; accepted 2 January 1996

Abstract

A study is described of the heterogeneous kinetics of Photosystem II (PSII) electron transport in osmotically swollen spinach chloroplasts ('blebs') on illumination by a series of laser flashes. The existence of a broad distribution of the number of plastoquinone molecules rapidly accessible for reduction by PSII is confirmed by chlorophyll fluorescence yield and electroluminescence measurements as a function of the number of preilluminating flashes. The oscillation of electroluminescence with flash number as a function of flash energy was used to calculate the best-fitting antenna-size distribution of the oxygen evolving PSII. The results suggest that, in blebs at least, electrogenic charge separation leading to electron transport from water to the plastoquinone pool is carried out by PSII β as well as PSII α.

Keywords: Photosystem II; Heterogeneity; Plastoquinone pool; Antenna size

1. Introduction

In the presence of DCMU the light-induced increase of the chlorophyll fluorescence yield in Photosystem II reflects a single photoreaction resulting in the photoreduction of Q_A, as originally proposed by Duysens and Sweers [1]. At rate-limiting light intensity the kinetics of the process are clearly biphasic [2], which has been attributed to the presence of two different types of PSII: PSII α and PSII β [3,4]. Both systems have a high quantum yield of Q_A photoreduction [5,6], so the kinetic difference is due to a different absorption cross section. The antenna size of PSII α is 2–3-times larger than that of PSII β. During the fluorescence induction the effective antenna size of PSII α further increases due to energy transfer between units, leading to a sigmoidal fluorescence rise curve, whereas PSII β centers behave as separate units and cause a simple exponential fluorescence increase. This is attributed to their different locations: PSII α is thought to be concentrated in the appressed membrane regions in the grana, while PSII β is located in the stroma-exposed membrane regions, interspersed among PSI [6].

The functional significance of PSII β has never been fully clarified. A heterogeneity in antenna size suggests a role in adaptation to the wide range of light intensities to which plants are exposed. Support for such a role comes from variations in the relative abundance of PSII β between sun and shade plants and plants grown at different light intensities [7,8]. However, various observations indicate that also electron transport by PSII β may be different from that by PSII α and suggest that PSII β is unable to reduce the plastoquinone pool [9,10]. If PSII β is active in electron transfer at all, the electron transfer pathway could be totally different, not involving quinones and not associated with a membrane potential [11,12]. Some data indicate that PSII β does evolve oxygen when lipophilic quinones are added as artificial electron acceptors [13,14]. It has been proposed that PSII β represents a transient, inactive stage in a continuous repair cycle triggered by irreversible photoinhibition of PSII [8]. This hypothesis might also account for the observed correlation with growth conditions, although the amount of PSII β normally present in non-photoinhibited material, about one-third of the reaction centers, seems wastefully large.

In the absence of DCMU, PSII photochemistry brings about the transfer of electrons from water to plastoquinone. When the plastoquinone pool becomes reduced the reoxi-

Abbreviations: DCBQ, 2,5-dichloro-*p*-benzoquinone; DCMU, 3-(3',4'-dichlorophenyl)-1,1-dimethylurea; EL, electroluminescence; LHCII, light harvesting complex of Photosystem II; PSI, Photosystem I; PSII, Photosystem II; Q_A and Q_B secondary electron acceptors of Photosystem II.

* Corresponding author. Fax: +31 71 5275819; e-mail: vangorkom@biophys.leidenuniv.nl.

PII S0005-2728(96)00006-0

dation of the electron acceptor Q_A^- is also inhibited and the chlorophyll fluorescence yield increases correspondingly. The long-known fact that photo-accumulation of Q_A^- follows the reduction of the pool much closer than redox equilibration would predict led Joliot et al. [15] to propose that only local equilibration in isolated domains can be attained and a wide distribution of pool sizes in different domains determines the measured kinetics. The most obvious support for this model came from the observation that the decrease of oxygen production due to accumulation of Q_A^- upon photo-reduction of the pool by a series of saturating flashes is not associated with a corresponding increase in 'misses' in the oscillation of oxygen yield with flash number. When PSII is illuminated by a series of saturating flashes the oxygen yield shows a damped oscillation with a maxima on flash numbers 3, 7, 11, etc. [16]. Kok et al. [17] proposed that each reaction center cycles through five redox states, now referred to as the 'S-states':

$$S_0 \Rightarrow S_1 \Rightarrow S_2 \Rightarrow S_3 \Rightarrow (S_4 \rightarrow) S_0 + O_2$$

The damping of the oscillation was attributed to imperfect single-turnover flashes: 'double hits' may be prevented by the use of sufficiently short flashes, but even with saturating flashes there are always some 'misses' because the stabilization of the charge separation after the flash fails, e.g., because Q_A was already in the reduced state.

If the fluorescence yield increase accompanying plastoquinone pool reduction is due to a dynamic redox equilibrium between Q_A and the pool as a whole, the probability of misses should increase correspondingly. Clearly, this is not observed in the oxygen sequence [15] and also the shape of the fluorescence rise curve is difficult to explain unless a broad distribution of pool sizes is assumed [18]. Joliot et al. [19] have argued that the number of plastoquinone molecules accessible to a PSII center is a statistically distributed value which changes only slowly ($t_{1/2} = 6$ s) because the high protein density in the membrane causes a fragmentation of the lipid space available for free diffusion of plastoquinone. Satisfactory agreement with percolation theory was obtained [20], and the lateral diffusion of plastoquinone in the thylakoid membrane was indeed found to be at least two orders of magnitude slower than in phosphatidylcholine membranes [21].

We have investigated the kinetics of S-state oscillation and pool reduction in osmotically swollen chloroplasts ('blebs'), where the reduction kinetics of the plastoquinone pool can be studied conveniently because its reoxidation by PSI is inhibited [22], and where the S-state oscillation can be probed conveniently by the electroluminescence (EL) technique [23]. In this way plastoquinone reduction and S-state oscillation could be detected by measuring chlorophyll fluorescence emission, so that the same apparatus, experimental conditions and material could be used. By comparison of measurements in the presence and absence of the artificial electron acceptor DCBQ, which fully reoxidizes Q_A^- between flashes, the effects of photoreduction of the plastoquinone pool were easily distinguished from other phenomena. Variations of the flash energy allowed the determination of the antenna sizes of the PSII units involved.

2. Materials and methods

Chloroplasts were isolated from laboratory-grown spinach. Freshly harvested leaves were depetiolated, washed and ground in a cooled blender in 50 mM Hepes (pH 7.5)/0.4 M NaCl/1 mM EDTA/0.2% (w/v) BSA. After filtration through a 25-μm mesh nylon cloth, chloroplasts were sedimented by 10 min centrifugation at 10000 $\times g$. The pellet was resuspended in 50 mM Hepes (pH 7.5)/0.15 M NaCl/5 mM $MgCl_2$ to a chlorophyll concentration of 2 mg/ml. The preparations were stored at 77 K until use. Blebs were formed by diluting the chloroplast suspension 400-fold in 1 mM Mops (pH 6.6)/1 mM $CaCl_2$. Where indicated the artificial PSII electron acceptor 2,5-dichloro-p-benzoquinone (DCBQ) was added. The measurements were performed about 10 min after dilution at about 18°C. For each measurement a fresh sample was taken (successive points in a flash series thus result from mutually independent experiments). Each point is the average of two measurements.

The measuring cuvette, which was placed in the focus of an ellipsoidal mirror for efficient collection of emitted light, consisted of two 10×10 mm platinum electrodes spaced at 2 mm by the surrounding glass sides. Slits next to one of the electrodes allowed sample replacement by an automatic stopped-flow system. Two opposite sides could be illuminated via small holes in the mirror; one was used for the actinic flashes and one for the measuring beam to probe the fluorescence yield. Emitted light was reflected by the mirror, through a Balzers 686 nm interference filter and a Schott RG665 nm cut-off filter, on a photomultiplier which was shut off during the excitation flashes by an electronic gate. The excitation flashes were obtained from a Nd-YAG laser (10 Hz, 532 nm, 20 ns half-width) and filtered by a Balzers Calflex C and Corning CS 4-96.

For electroluminescence (EL) measurements, at 500 μs after the last flash a 140 μs square pulse of 330 V was applied to the electrodes, resulting in an electrical field strength of 1650 V/cm in the cuvette. The signal from the photomultiplier, recorded by a Datalab 905 transient recorder and fed into a microcomputer, was integrated from 25 μs to 125 μs after the onset of the pulse.

For fluorescence yield measurements, after the last flash a shutter was opened to admit a weak probing beam, filtered by a Calflex C and a CS 4-96 and modulated by a photoelastic modulator (Hinds International) placed between crossed polarizers. The signal from the photomultiplier, first demodulated by a lock-in amplifier and then

recorded as above, was integrated from 50 ms to 150 ms after the last flash. The integrated fluorescence signal as a function of flash number was normalized for zero flashes.

The accuracy of the integrated fluorescence and EL values appeared to be limited by a relative error of about 2% root-mean-square deviation. Fitting was therefore performed by minimizing the RMS *relative* difference between the simulated and the measured values, using the NAG Library routine E04JAF. The program allowed global fitting of several data-sets, variables could be made constant/free, upper and lower bound, set-dependent/independent and heterogeneous/homogeneous. In order to determine a distribution of values of a variable, the simulation is calculated for a series of fractions with successive, fixed values of the variable and the size of each fraction is a fit variable. The resolution of the distribution is rather low because of the limited number of fractions which could be handled, especially when many other variables were set free as well. When a broad distribution, extending over many fractions, is obtained, the procedure tends to produce alternatingly high and low values for successive fractions. This is an inherent instability of the method, appearing when the difference between calculated signals from successive fractions does not much exceed the noise in the data. To cope with this problem, the distributions shown in Fig. 3 were filtered by plotting not the actually fitted size $y(n)$ of each fraction n, but $0.5\ y(n) + 0.25\ y(n-1) + 0.25\ y(n+1)$. The results obtained after filtering were essentially independent of the initial values used on entry of the fitting subroutine. The same fitting instability does not play an important role in the narrow antenna-size distributions of Fig. 7. In that case the fitted values are shown without smoothing.

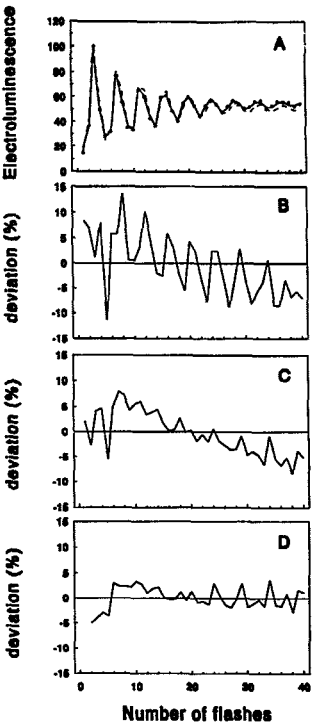

Fig. 1. Relative electroluminescence induced by an 0.14 ms electrical field pulse applied at 0.5 ms after a variable number of single-turnover flashes fired at 10 Hz in the presence of 50 μM DCBQ. Dashed line (deviations shown in B): best fit according to the Kok-model, 8.3% misses. Deviations in C: reversible inactivation of S_3 (39% inactivation, 71% reactivation). Solid line, with deviations shown in D: best fit disregarding the first flash and assuming a fixed EL increase per electron transported. Values obtained with this fit: misses 0%; S_3 inactivation 38.6%; S_3 reactivation 75.5%; EL S_0-S_3 22.2, 14.2, 25.9 and 100; EL increase/electron 0.0037.

3. Results

3.1. S-state turnover

Fig. 1A shows the amplitude of EL signals measured on a suspension of blebs as a function of the number of preilluminating single-turnover flashes, in the presence of the artificial electron acceptor DCBQ. The electrical pulse was applied at 0.5 ms after the last flash to minimize the relative contribution of non-oscillating centers [23] and the emission during the first 25 μs of the pulse was discarded to avoid a contribution by EL from PSI [22]. The pronounced period four oscillation with flash number was analysed in detail in Ref. [23]. It is similar to that of the oxygen yield, because the largest signal is observed after a flash fired in S_3, but the contributions by the other S-states are substantial. Fitting the period four oscillation with flash number requires an S-state dependent EL contribution and some variables to quantify the S-state turnover according to the Kok model [17]. The kinetic parameters of the S-state turnover are determined by the damping and period of the oscillation. In view of the short flash duration and the absence of measuring light during the flash sequence, double hits could be excluded. The probability of misses alone is clearly not enough to describe the oscillation pattern (dashed line, deviations shown in Fig. 1B). The amplitude of the oscillation decreases more rapidly than can be explained by the maximum amount of misses allowed by the period of the oscillation, as noted before [25]. The replacement of Kok's miss parameter by an irreversible inactivation of a fraction of the centers on each flash [25] was not satisfactory. The assumption of a 'reversible inactivation of S_3' [26], which entails two extra fit variables, allowed a close fit of the oscillation patterns. Typical values for S_3 inactivation and reactivation were 35 and 75%, respectively, with very few S-state independent misses. This is probably not realistic and shows again that

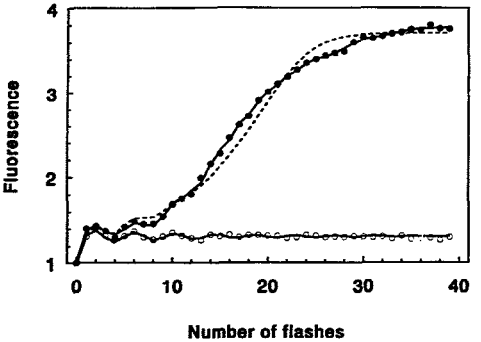

Fig. 2. Relative chlorophyll fluorescence yield in blebs at 50–150 ms after a variable number of single-turnover flashes fired at 10 Hz, in the absence (solid circles) and presence (open circles) of 50 μM DCBQ. The lines show the best-fitting simulation with a distribution of acceptor pool sizes as explained in the text; the dashed line in is the best fit obtained for a homogeneous plastoquinone pool size.

the details of S-state turnover are not quantitatively understood. We will use the 'reversible S_3 inactivation' only by lack of a more plausible model which allows an accurate fit. From preillumination-deactivation experiments as described in Ref. [23] it was clear that all centres started in the state S_1 (not shown). The pattern of deviations (Fig. 1C) shows a small linear increase of the EL signal with flash number. If this is accounted for by arbitrarily assuming a fixed increase of the EL signal for each electron transported and the first flash is disregarded in view of the possibly smaller contribution by non-oscillating centers [23], the residuals are reduced nearly to the noise in the data (Fig. 1D).

3.2. Pool size distribution

The chlorophyll fluorescence yield of the same material was measured in the same conditions as a function of the number of preilluminating single-turnover flashes, both in the absence and in the presence of the artificial electron acceptor DCBQ (Fig. 2, solid circles and open circles, respectively). The measurement started 50 ms after the last flash, after equilibration of secondary electron transfer reactions of PSII, and ended at 150 ms after the flash, before significant S-state deactivation or reoxidation of the plastoquinone pool took place. The large increase of the fluorescence yield after many flashes in Fig. 2 (solid circles) is attributed to the accumulation of Q_A^- when the plastoquinone pool becomes exhausted, which could be completely prevented by addition of the artificial electron acceptor DCBQ (Fig. 2, open circles). Oscillations with flash number are attributed to the four different S-states and the two Q_B-states. The larger difference between zero and one flash is attributed to a minor fraction of 'inactive centers', which are unable to proceed beyond the state $S_2Q_A^-$ [24].

In order to verify if these data can be explained quantitatively by the above interpretation with reasonable values of all parameters involved, computer simulations were carried out and optimized by mean-square minimalization of the relative difference between simulated and measured values. The lines in Fig. 2 indicate a simultaneous fit of the data with and without DCBQ, obtained as follows. To accommodate the fluorescence increase due to inactive centers a separate variable was included. They were assumed to have the same fluorescence properties as normal centers in S_1.

The relative fluorescence yield (F/F_{max}) as a function of the fraction of Q_A in the oxidized state (q) was calculated according to Ref. [27] using the equation:

$$F/F_{max} = 1 - q/((F_{max}/F_v)_i - p(1-q))$$

in which $(F_{max}/F_v)_i$ was treated as the only S_i-state dependent fit variable. F_{max} is the fluorescence corresponding to all Q_A reduced and the variable fluorescence $(F_v)_i$ is $F_{max} - (F_0)_i$, with $(F_0)_i$ the fluorescence corresponding to all Q_A oxidized. If the reaction centers do not quench fluorescence when Q_A is reduced, as concluded in Ref. [5], $(F_v/F_{max})_i$ is the efficiency of excitation trapping in 'open' PSII (Q_A in the oxidized state). This parameter is thought to depend on the S-state dependent local electrostatic field at the site of charge separation [28]. For S-state kinetics as in Fig. 1, its fitted values were 0.710, 0.719, 0.692 and 0.676 for S_0, S_1, S_2 and S_3, respectively. These values presumably include some dependence on the redox state of Q_B, which was disregarded in the model.

The parameter P is the probability of excitation transfer from a 'closed' PSII (where Q_A is in the reduced state) to another PSII [29] (corresponding to ω in Ref. [27]). The best-fitting value was 0, but the fit was quite insensitive to the value of P. When a value of 0.8 was imposed, the resulting delay in the calculated fluorescence rise as a function of flash number was compensated in the fit by a marginal increase of the small pool sizes and the value of K (see below) was not changed.

The only difference between the fits of Fig. 2 in the absence (solid circles) and in the presence of DCBQ (open circles) was that in the latter complete reoxidation of Q_A^- between flashes was assumed. In the absence of DCBQ, Q_A was assumed to be in one-electron redox equilibrium with the plastoquinone pool, disregarding the two-electron gate Q_B, and q, the fraction of Q_A in the oxidized state, was calculated from the equation:

$$q = K/(K + r)$$

in which K is the apparent equilibrium constant and r is the plastoquinol/plastoquinone ratio. The value of r follows from the number of electrons already transferred to the pool, calculated from S-state turnover, and the pool size. The best-fitting simulation with a homogeneous pool

size was clearly not acceptable, as illustrated by the dashed line in Fig. 2 and the fitted value of the equilibrium constant ($K = 7$) was much smaller than expected [30]. Also two and even three populations of PSII with different fitted pool sizes could not satisfactorily describe the shape of the fluorescence increase with flash number (not shown). When a larger number of fractions with a fixed range of pool sizes was allowed and their relative contributions fitted, a broad and asymmetrical distribution from 4 to 15 plastoquinone molecules with a maximum at 7 was obtained (Fig. 3A, solid circles). The shoulder at 12, related to the irregularities at flash number 28–30 in Fig. 2, is probably not significant. The value of the equilibrium constant in this fit was $K = 32$, i.e., larger than the size of the acceptor pool. Larger values of K led to equivalent fits. The accumulation of Q_A^- in one domain must be practically a step function, occurring when the locally available plastoquinone has been exhausted. This explains why the fit results are independent of the simplifying assumptions made about electron transfer to the pool. For simplicity and speed of computation we assumed a one-electron equilibrium between Q_A and its local acceptor pool. Lavergne et al. [20] took into account that plastoquinol is a two-electron carrier. The open circles in Fig. 3B show the pool size distribution as derived by an elaborate procedure in Ref. [20] from the oxygen measurement shown in Fig. 8 of Ref. [19], while the solid circles indicate the distribution we obtain by a direct fit of the same data. Although the approach and the inherent assumptions are different, the result is similar. The last point differs because Lavergne et al. [20] subtracted the small residual oxygen evolution remaining after pool reduction. This distribution of pool sizes is similar to that of Fig. 3A (solid circles).

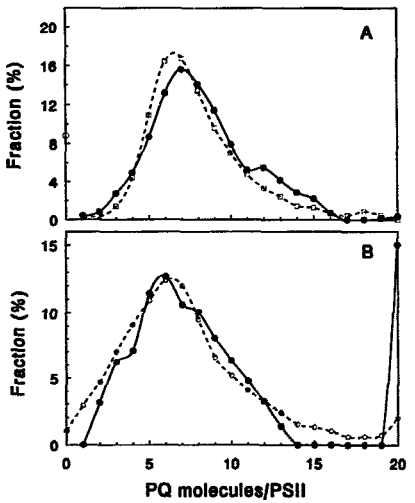

Fig. 3. (A) Best-fitting distributions of acceptor pool sizes obtained by the fluorescence fit of Fig. 2 (solid circles) and the EL fit of Fig. 4 (open squares), smoothed as described in Section 2. The open circle at a pool size of zero indicates the amount of inactive centers applied for the fluorescence fit. (B) Best-fitting size distribution (solid circles) of the plastoquinone pool for the oxygen flash yield sequence in chloroplasts reported by Joliot et al. (their Fig. 8) [19]. Fitted variables: initial $S_1 = 100\%$; misses = 8.4%; double hits = 2.2%; $K_{eq} = 52$; fractions containing 1–20 plastoquinone per PSII (the last fraction, accounting for the small continued O_2 evolution, may be replaced by 1.1% reoxidation of plastoquinol between flashes). Open circles: distribution derived by Lavergne et al. from the estimated accumulation of Q_A^- during the same experiment [20].

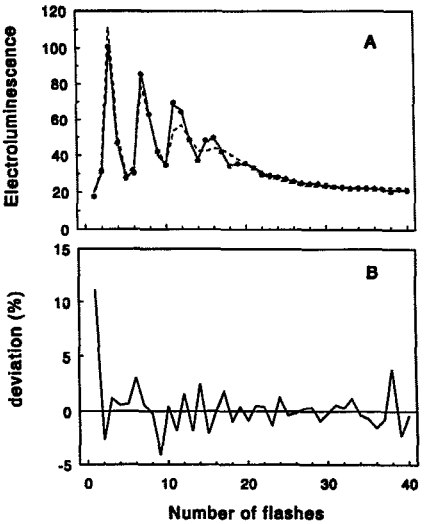

Fig. 4. Relative electroluminescence yield during a 0.14-ms electrical field pulse applied at 0.5 ms after a variable number of single-turnover flashes fired at 10 Hz as in Fig. 1, but without the addition of DCBQ. The lines show the best-fitting simulation with a distribution of acceptor pool sizes (shown in Fig. 3A, open squares). The deviations are shown in B. Fitted variables as in Fig. 1 and Fig. 2 (misses 1.1%; S_3 inactivation 34.6%; S_3 reactivation 77.4%; K_{eq} 30.6; EL contribution S_0-S_3 18.5, 14.3, 23.0 and 100; EL S_2Q^-/S_3Q^- 17.7; EL increase per electron 0.028).

Fig. 4 shows the EL signals under the same conditions as in Fig. 1 with the same batch of material but without DCBQ. After complete reduction of the plastoquinone pool and disappearance of the oscillation large signals are still observed, presumably because the accumulation of Q_A^- enhances electric field-induced charge recombination and half of the centers are in a high S-state. To simulate these EL data the same kinetic parameters of S-state turnover as in Fig. 1 and of pool reduction as in Fig. 2 were used and almost identical values were obtained. This result does not support the conclusion of Delrieu and Rosengard [25] that the period four oscillation of the fluorescence yield at 80 ms after the flash is due to a small fraction of centers with

unusual S-state turnover properties. The fitted relative amplitudes of EL signals after a flash fired in S_0, S_1, S_2 and S_3 were 18.5, 14.3, 23.0 and 100. That of centers which were in $S_2Q_A^-$ or $S_3Q_A^-$ before the flash was 17.7 (no distinction between these states could be made); centers in $S_0Q_A^-$ or $S_1Q_A^-$ before the flash were assumed not to contribute to the EL.

Again a homogeneous pool size did not allow an acceptable fit: the decrease of the amplitude of the oscillation upon reduction of the pool was not accompanied by a corresponding increase of misses. The best-fitting distribution of pool sizes (Fig. 3A, open squares) was similar to that obtained from the fluorescence yield measurements. Again a fixed increase of the EL for each electron transported had to be assumed, as in Fig. 1, but with a larger value (0.028). Moreover, the occurrence of such an increase was obvious already without fitting in EL measurements on chloroplasts, and also on blebs when no divalent cations are added (not shown). It was insensitive to uncouplers and its origin is not clear. The absolute values of the integrated EL were substantially smaller in the presence of DCBQ than in its absence. Since this could not be accounted for by the extent of fluorescence quenching by DCBQ, it was presumably due to accelerated reoxidation of Q_A^-

3.3. Antenna size distribution

The experiments described above show that all oscillating EL comes from PSII centers connected to the plastoquinone pool. Saturating flashes were used and any heterogeneity in the antenna size of the PSII involved would be obscured. It was shown in Refs. [5] and [6] that the smaller PSII β has an even higher yield of stable charge separation in a saturating flash than PSII α. In order to investigate the participation of PSII β in electron transport from water to plastoquinone or to DCBQ, the oscillation of EL with flash number was measured as a function of the energy of the flashes, both with and without DCBQ (Figs. 5 and 6, respectively). For the measurements in the absence of DCBQ the values beyond flash nr. 10 were discarded, so that limitation by the acceptor pool could be disregarded in the fit. Saturation with flash energy (I) was assumed to be a single exponential ($1-\exp(-I/I_{sat})$) and the characteristic 'saturation' energy I_{sat}, at which ($1-1/e$) of the maximum amount of charge separation occurs, was the fitted variable, expressed in the same relative units as the flash energy used with each flash series (here: % transmittance of the neutral density filters placed in the laser beam). The dashed lines in Fig. 5 show the best fit assuming a single value of I_{sat}, corresponding to a homogeneous antenna size. Especially at 20% and at 13% flash energy the deviation from the data is clear.

The best-fitting distribution of saturation energies was obviously bimodal, both with and without DCBQ, as shown in Fig. 7 solid and open circles, respectively. In the

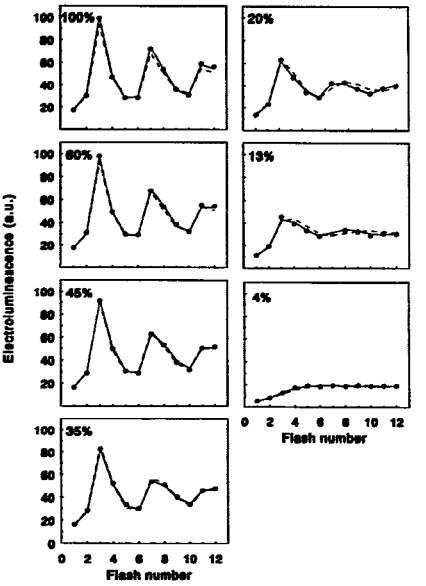

Fig. 5. Electroluminescence measurements in the presence of 50 μM DCBQ as in Fig. 1, carried out at different flash energies (% transmittance of the neutral density filters as indicated). The lines show the best-fitting simulation of the complete data set with a distribution of antenna sizes as explained in the text; the dashed line is the best fit obtained for a homogeneous antenna size.

presence of DCBQ half of the oscillating EL signals is saturated at about 2.3-times lower flash energy than the other half, which corresponds to the difference between PSII α and PSII β centers as proposed by Melis and Homann [4]. The absorption cross-section or antenna size is proportional to the reciprocal of the saturation energy, so the relatively smaller contribution of the high energy peak in the absence of DCBQ suggests a smaller contribution by PSII β, as might have been expected. The fits may also indicate that DCBQ causes a slight shift to higher energy of both peaks, as expected due to excitation quenching by DCBQ. However, the detailed shape of the distributions should not be over-interpreted; considerable variations of the distributions could be imposed without much increase of the minimum deviation between fit and data; the only definite conclusion was that the distribution must have two well-separated maxima with comparable amplitudes, both in the presence and in the absence of DCBQ.

When only two antenna sizes were allowed, the best fitting saturation energies were 5.5 and 15.5% in the absence of DCBQ (open squares in Fig. 7) and 7.5 and 18% in its presence (solid squares). The relative amount of β-centers was 38% and 50%, in the absence and presence of DCBQ, assuming equal EL yields of α and β centers. This assumption is probably not correct. Quenching by

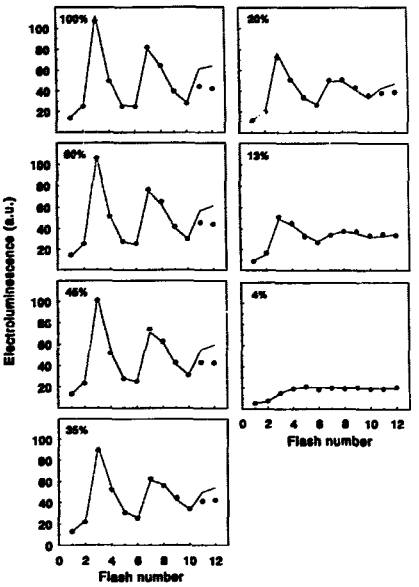

Fig. 6. Electroluminescence measurements in the absence DCBQ as in Fig. 4, carried out at different flash energies, indicated in each frame by the % transmittance of the neutral density filters used. The lines show the best-fitting simulation disregarding flash numbers 11 and 12, with a distribution of antenna sizes as explained in the text.

DCBQ will affect the smaller β units less than PSII α. Besides, the S-state dependence of EL appeared to be different. For homogeneous S-state turnover kinetics different EL contributions of the successive S-states were obtained for PSII α and PSII β. Conversely, if those contributions were kept homogeneous, the kinetic parameters were α/β-dependent (with fewer misses in β than in α, in agreement with Ref. [5]). Probably both are α/β-dependent, but erratic fitting results were obtained when heterogeneity was allowed simultaneously in the kinetic parameters and the S-state dependent contributions to the measured EL signal. More precise data or additional evidence will be needed to proceed further.

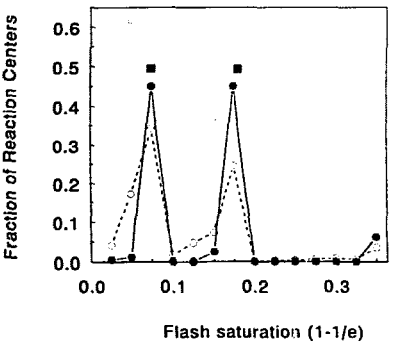

Fig. 7. Best-fitting distributions of saturation energies for the EL data of Fig. 5 (solid circles, with DCBQ) and those of Fig. 6 (open circles, without DCBQ). The squares indicate the fitted amounts and saturation energies when only two fractions were allowed.

4. Discussion

The results reported here show that the oscillating EL signals come from PSII centers that are involved in electron transport from water to the plastoquinone pool. The absorption cross-section of those centers comes in two discrete sizes apparently corresponding to the α/β heterogeneity of Melis and Homann [4]. The conclusion that β centers carry out electron transport to the plastoquinone pool is hard to reconcile with earlier evidence indicating that these centers are not connected to the two-electron gate Q_B [9,10]. There are three solutions: (1) what we see is not PSII β; (2) our conditions reactivate PS IIβ; (3) PSII β reduces plastiquinone without a two-electron gate.

Firstly, the centres with β-type antenna size might be α-centres stripped of their peripheral LHC II by the blebbing process, in analogy to what has been proposed to occur upon short heat-treatment [31] and the true β-centers might escape detection in our measurements because they do not oscillate and/or are not sensitive to a membrane potential [32]. This would imply that our preparations should contain large amounts of detached LHCII or an increased antenna size of the centers left behind. However, the overall F_{max}/F_0 ratio of four does not suggest either. Secondly, electron transport from water to plastoquinone might be reactivated in PSII β by the blebbing process. This seems unlikely. We have no evidence that the total flash yield of oxygen increases and a redistribution of plastoquinone is unlikely in view of the unchanged pool size (Fig. 3) and earlier evidence for a normal plastoquinone content of stroma lamellae [33,34]. Thirdly, one might design schemes to explain plastoquinone reduction by PSII β without two-electron gate, involving a cooperation between reaction centres, perhaps in association with the cytochrome b/f complex [35]. The problem with this interpretation, however, is that electrons arriving at PSI seem to be limited by the two-electron gate [36]. On the other hand, some electrons do arrive after a single flash, and the hypothesis that this is due to the presence of some (30%) Q_B^- in the dark [36,37] has never been proven. In fact it is inconsistent with the absence of a corresponding absorbance change at 325 nm after the first flash (e.g., Ref. [23]).

We conclude that all three interpretations would require further research to become acceptable and none of them can be ruled out at this stage. The key question is, if plastoquinone reduction by the β-type PSII described here proceeds via the two-electron gate Q_B. The finding that the

EL signal is dependent on the redox state of Q_B [38] opens the possibility for a further study of this question.

Acknowledgements

This work was supported by the Netherlands Foundation for Chemical Research (SON), financed by the Netherlands Organization for Scientific Research (NWO).

References

[1] Duysens, L.N.M. and Sweers, H.E. (1963) in Studies in Microalgae and Photosynthetic Bacteria pp. 353–372, University of Tokyo Press, Tokyo.
[2] Doschek, W.W. and Kok, B. (1972) Biophys. J. 12, 832–838.
[3] Melis, A. and Homann, P.H. (1975) Photochem. Photobiol. 21, 431–437.
[4] Melis, A and Homann, P.H. (1976) Photochem. Photobiol. 23, 343–350.
[5] Thielen, A.P.G.M. and Van Gorkom, H.J. (1981) Biochim. Biophys. Acta 637, 439–446.
[6] Thielen, A.P.G.M. and Van Gorkom, H.J. (1981) Biochim. Biophys. Acta 635, 111–120.
[7] Anderson, J.M. and Melis, A. (1983) Proc. Natl. Acad. Sci. USA 80, 745–749.
[8] Melis, A. (1991) Biochim. Biophys. Acta 1058, 87–106.
[9] Thielen, A.P.G.M. and Van Gorkom, H.J. (1981) FEBS Lett. 129, 205–209.
[10] Hideg, E. and Demeter, S. (1988) Z. Naturforsch. 43c, 596–600.
[11] Black, M.T., Brearley, T.H. and Horton, P. (1986) Photosynth. Res. 8, 193–207.
[12] Govindjee (1990) Photosynth. Res. 25, 151–160.
[13] Albertsson, P.-A. and Shi-Gui, Y. (1988) Biochim. Biophys. Acta 936, 215–221.
[14] Nedbal, L., Gibas, C. and Whitmarsh, J. (1991) Photosynth. Res. 30, 85–94.
[15] Joliot, P., Lavergne, J. and Béal, D. (1990) in Current Research in Photosynthesis (Baltscheffsky, M., ed.), Vol. II, pp. 879–882, Kluwer, Dordrecht.
[16] Joliot, P. and Kok, B. (1975) in Bioenergetics of Photosynthesis (Govindjee, ed.) pp. 387–412, Academic Press, New York.
[17] Kok, B., Forbush, B. and McGloin, M. (1970) Photochem. Photobiol. 11, 457–475.
[18] Hsu, B.-D. (1992) Biochim. Biophys. Acta 1140, 30–36.
[19] Joliot, P., Lavergne, J. and Béal, D. (1992) Biochim. Biophys. Acta 1101, 1–12.
[20] Lavergne, J., Bouchaud, J.-P. and Joliot, P. (1992) Biochim. Biophys. Acta 1101, 13–22.
[21] Blackwell, M., Gibas, C., Gygax, S., Roman, D. and Wagner, B. (1994) Biochim. Biophys. Acta 1183, 533–543.
[22] Vos, M.H. and Van Gorkom, H.J. (1988) Biochim. Biophys. Acta 934, 293–302.
[23] Vos, M.H., Van Gorkom, H.J. and Van Leeuwen, P.J. (1991) Biochim. Biophys. Acta 1056, 27–39.
[24] Lavergne, J. and Leci, E. (1993) Photosynth. Res. 35, 323–343.
[25] Delrieu, M.-J. and Rosengard, F. (1987) Biochim. Biophys. Acta 892, 163–171.
[26] Van Leeuwen, P.J., Heimann, C. and Van Gorkom, H.J. (1993) Photosynth. Res. 38, 323–330.
[27] Paillotin, G. (1976) J. Theor. Biol. 58, 237–252.
[28] Dau, H. (1994) Photochem. Photobiol. 60, 1–23.
[29] Joliot, A. and Joliot, P. (1964) C.R. Acad. Sci. Paris 258, 4622–4625.
[30] Diner, B.A. (1977) Biochim. Biophys. Acta 460, 247–258.
[31] Sundby, C., Melis, A., Mäenpää, P. and Andersson, B. (1986) Biochim. Biophys. Acta 851, 475–483.
[32] Meiburg, R.F., Van Gorkom, H.J. and Van Dorssen, R.J. (1984) Biochim. Biophys. Acta 765, 295–300.
[33] Jennings, R.C., Garlaschi, F.M. and Gerola, P.D. (1983) Biochim. Biophys. Acta 722, 144–149.
[34] Chapman, D.J. and Barber, J. (1986) Biochim. Biophys. Acta 850, 170–172.
[35] Joliot, P. and Joliot, A. (1983) in The Oxygen Evolving System of Photosynthesis (Inoue, Y., Crofts, A.R., Govindjee, Murata, N., Renger, G. and Satoh, K. eds.), pp. 357–368, Academic Press, New York.
[36] Bouges-Bocquet, B (1973) Biochim. Biophys. Acta 314, 250–256.
[37] Fowler, C.F. (1977) Biochim. Biophys. Acta 459, 351–363.
[38] Hemelrijk, P.W. and Van Gorkom, H.J. (1996) Photosynth. Res., in press.